Radiographic, magnetic resonance imaging, computed tomographic, and rhinoscopic features of nasal aspergillosis in dogs

Jimmy H. Saunders, DMV, PhD; Cécile Clercx, DMV, PhD; Frédéric R. Snaps, DMV, PhD; Martin Sullivan, DVM, PhD; Luc Duchateau, DVM, PhD; Henri J. van Bree, DMV, PhD; Robert F. Dondelinger, MD, PhD

Objective—To determine radiographic, magnetic resonance imaging (MRI), computed tomography (CT), and rhinoscopic features of nasal aspergillosis in dogs.

Design—Prospective study.

Animals—15 client-owned dogs.

Procedure—All dogs had clinical signs of chronic nasal disease; the diagnosis of nasal aspergillosis was made on the basis of positive results for at least 2 diagnostic tests (serology, cytology, histology, or fungal culture) and detection of typical intrasinusal and intranasal fungal colonies and turbinate destruction via rhinoscopy. Radiography, MRI, and CT were performed under general anesthesia. Rhinoscopy was repeated to evaluate lesions and initiate treatment. Findings of radiography, MRI, CT, and rhinoscopy were compared.

Results—MRI and CT revealed lesions suggestive of nasal aspergillosis more frequently than did radiography. Computed tomography was the best technique for detection of cortical bone lesions; the nature of abnormal soft tissue, however, could not be identified. Magnetic resonance imaging allowed evaluation of lesions of the frontal bone and was especially useful for differentiating between a thickened mucosa and secretions or fungal colonies; however, fungal colonies could not be differentiated from secretions. Rhinoscopy allowed identification of the nature of intranasal and intrasinusal soft tissue but was not as useful as CT and MRI for defining the extent of lesions and provided no information regarding bone lesions.

Conclusions and Clinical Relevance—The value of CT and MRI for diagnosis of nasal aspergillosis was similar and greater than that of radiography. Rhinoscopy is necessary because it is the only technique that allows direct visualization of fungal colonies. (*J Am Vet Med Assoc* 2004;225:1703–1712)

Up to 34% of dogs with chronic nasal disease have nasal aspergillosis.[1-3] *Aspergillus fumigatus* is the most commonly isolated species; it is ubiquitous in the environment and is most commonly found in compost, stables, and barns.[1,2] Dolichocephalic and mesaticephalic dogs are most commonly affected[1,4]; however, a definite breed predilection has not been detected.[4,a,b] Male dogs appear to be at greater risk than female dogs.[4] The age at first examination ranges from 9 months to 14 years (mean, 4 years); 80% of affected dogs are younger than 8 years of age.[a,b]

The diagnosis of nasal aspergillosis in dogs is made on the basis of history; clinical signs; physical examination and rhinoscopic findings; and results of serology, cytology, histology, imaging studies (radiography and **computed tomography [CT]**), and fungal culture. The diagnosis of aspergillosis is made on the basis of at least 2 (preferably 3) positive test results.[5]

The radiographic, computed tomographic, and rhinoscopic features of nasal aspergillosis have been described.[6-8] With radiography and CT, the diagnosis is made mainly on the basis of the cavitated appearance of the nasal cavity and the presence of hyperostotic bone, whereas with rhinoscopy, the diagnosis is made on the basis of direct visualization of fungal colonies in nasal cavities lacking turbinates.[6,7] Computed tomography is more sensitive than radiography for the diagnosis of nasal aspergillosis, particularly in dogs with lesions restricted to the rostral half of the nasal cavities.[9]

Magnetic resonance imaging (MRI) is superior to CT for evaluation of soft tissue structures and is widely used in humans for evaluation of the nasal cavities, paranasal sinuses, and surrounding structures.[10-12] Recently, MRI has been used for diagnosis of diseases of the head (principally brain abnormalities) in small animals[13-16]; however, studies[16-18] in which MRI was used to evaluate animals with nasal disease are limited. Results of 1 study[17] suggested that MRI was more useful than CT for assessment of intracranial invasion of nasal neoplasms, anatomic features, and secondary pathologic lesions attributed to the neoplasm. A clinical report[18] revealed the usefulness of MRI for evaluation of intracranial (1 dog) and periorbital (1 cat) invasion of a nasal neoplasm. To the authors' knowledge, no detailed study comparing MRI features of nasal aspergillosis in dogs with those detected via CT and radiography has been performed. The purpose of the study reported here was to determine radiographic, MRI, CT, and rhinoscopic features of nasal aspergillosis in dogs.

Materials and Methods

The study was approved by the Ethical Committee of the University of Liège. Fifteen dogs with nasal aspergillosis

From the Departments of Medical Imaging (Saunders, van Bree) and Physiology, Biochemistry, and Biometrics (Duchateau), Faculty of Veterinary Medicine, Ghent University, 9820 Merelbeke, Belgium; the Department of Veterinary Medical Sciences, Faculty of Veterinary Medicine (Clercx, Snaps), and the Department of Medical Imaging, University Hospital Center (Dondelinger), University of Liège, 4000 Liège, Belgium; and the Department of Veterinary Clinical Sciences, University of Glasgow, Bearsden, Glasgow G61 1QH, Scotland (Sullivan).

Address correspondence to Dr. Saunders.

Unauthenticated | Downloaded 09/25/23 10:50 PM UTC

were included in the study (3 Labrador Retrievers, 2 Golden Retrievers, 2 Rottweilers, 2 Afghan Hounds, 1 Basset Hound, 1 German Shepherd Dog, 1 Belgian Shepherd, 1 Bull Terrier, 1 Newfoundland, and 1 mixed-breed dog). Age ranged from 1 to 8 years (mean, 3.6 years); there were 9 males and 6 females. All dogs had a history of nasal disease of > 2 months' duration and had been referred for further diagnostic investigation. All dogs underwent physical examination, and blood samples were obtained for serologic testing for anti-*Aspergillus* antibodies. For rhinoscopy, dogs were sedated with medetomidine (25 to 35 µg/kg [11.4 to 15.9 g/lb], IM) or acepromazine (0.025 to 0.05 mg/kg [0.011 to 0.023 mg/lb], IM) and methadone (0.2 to 0.4 mg/kg [0.09 to 0.18 mg/lb], IM). Anesthesia was induced with thiopental (5 to 10 mg/kg [2.3 to 4.5 mg/lb], IV) or propofol (2 to 6 mg/kg [0.9 to 2.7 mg/lb], IV) and maintained with isoflurane in oxygen. The nasal cavities and frontal sinuses were explored by use of a rigid endoscope[c] or a pediatric bronchoscope[d] specifically designed for endoscope-guided debridement, fluid infusion, and retrograde evaluation of the nasopharynx. Rhinoscopic images of the nasal cavities and frontal sinuses were obtained. During rhinoscopy, swab, brush, and biopsy specimens were collected for microbial culture, cytologic examination, and histologic examination, respectively. A definitive diagnosis of aspergillosis was made on the basis of positive results for at least 3 diagnostic tests including direct visualization of fungal colonies via rhinoscopy.

Three to 7 days after rhinoscopy, each dog was anesthetized for radiography, MRI, and CT. Owners of all dogs were informed about the potential risks of these examinations and gave their consent to perform them. Anesthesia was induced with droperidol and fentanyl (0.08 mg/kg [0.036 mg/lb], IV) and thiopental (5 to 10 mg/kg, IV) and maintained with halothane in oxygen in 12 dogs. In 3 dogs, anesthesia was induced with droperidol and fentanyl (0.08 mg/kg, IV) and maintained with pentobarbital (5 to 15 mg/kg [2.3 to 6.8 mg/lb], IV).

Radiography—Dorsoventral and lateral radiographic views of the entire skull, a dorsoventral (intraoral) radiographic view of the nasal cavities and maxilla, and a rostrocaudal radiographic view of the frontal sinuses were obtained by use of a 600-mA, 150-kv (peak) x-ray unit[e] with a focal distance of 100 cm. Orthochromatic films were used in combination with rare earth intensifying screens.[f]

MRI—Magnetic resonance imaging was performed after radiography. Eight dogs were evaluated by use of a 1.5T superconductive unit,[g] and 7 dogs were evaluated by use of a 1T superconductive unit.[h] All MRIs were performed as multisection, spin-echo studies. The T1-weighted images were obtained with a TR of 300 to 620 milliseconds and a TE of 10 to 15 milliseconds. The T2-weighted images were obtained with a TR of 2,800 to 5,200 milliseconds and a TE of 78 to 126 milliseconds. Postcontrast T1-weighted images were obtained within 10 minutes after administration of a 2mM solution of gadopentate dimeglumine[i] (0.2 mL/kg, IV). The acquisition matrix varied from 256 × 192 to 256 × 224 to 512 × 320. Transverse and dorsal plane images were obtained in all dogs, and sagittal plane images were obtained in 5 dogs. Contiguous 4-mm-thick sections were obtained. To improve the signal-to-noise ratio, a surface coil was used.

CT—Computed tomography was performed after MRI. A fourth-generation helical CT unit[j] was used. Dogs were positioned in ventral recumbency. Transverse slices from the caudal aspect of the frontal sinuses to the nares were acquired. Technical settings were 110 kv (peak), 125 mA, pitch of 1.5, index of 3, and slice thickness of 4 mm. Examinations before and after administration of a bolus of iohexol[k] (700 mg/kg [318 mg/lb], IV) were performed. The acquisition time was approximately 4 minutes. Hard copies of the images were printed with a bone window (window width = 3,500; window level = 500) and a soft tissue window (window width = 340; window level = 25). Reformatted dorsal plane images were also obtained.

Imaging findings—Various features were evaluated via the 3 imaging techniques. The extent of lesions (rostral half of the nasal cavity, all parts of the nasal cavity, and nasal cavity and frontal sinus) and whether they were unilateral or bilateral were evaluated. The nasal cavities were evaluated for degree of turbinate destruction (none, minimal, moderate, or severe), presence of abnormal soft tissue (none, minimal, moderate, or large amounts), presence of a rim of soft tissue lining the nasal cavities (ie, thickened mucosa), presence of abnormal soft tissue at the nasofrontal ostium, presence of a round soft tissue mass, mineralization of contents of the nasal cavity, presence of a foreign body, appearance of bone (normal, hyperostotic, lytic, or mixed pattern), lysis of the cribriform plate, and destruction of the nasal septum (only the bony portion for radiography). For the purposes of our study, abnormal soft tissue referred to exudates, fungal colonies, necrotic nasal mucosa, and mucosal edema that had a radiographic, MRI, and CT appearance compatible with that of soft tissue. Computed tomography is the optimal imaging technique for the evaluation of the frontal sinuses because of its ability to discriminate the natural contrast between air and bone; therefore, CT was considered the gold standard for the evaluation of the frontal sinuses in our study. The frontal sinuses were evaluated for the presence of fluid or abnormal soft tissue, presence of a rim of soft tissue lining the frontal sinuses (ie, thickened mucosa), appearance of the frontal bone (normal, hyperostotic, lytic, or mixed pattern), extension of lesions to the periorbital region, presence of a round soft tissue mass, and mineralization of contents of the frontal sinus. The overall appearance of the nasal cavities was classified as cavitated, mass-like, nondestructive, or normal. For MRI, the signal intensities of abnormal soft tissue in the nasal cavities and frontal sinuses and the enhancement characteristics were recorded and compared with those of normal turbinate mucosa and brain parenchyma in the same dog. For CT, special attention was given to the identification of the nature of abnormal intranasal and intrasinusal soft tissue.

Rhinoscopic findings—The day after the imaging studies, all dogs underwent a second rhinoscopic examination and findings were recorded for comparison with findings of radiography, MRI, and CT. The extent of lesions (nasal cavity or nasal cavity and frontal sinus) and whether they were unilateral or bilateral; degree of turbinate destruction (none, minimal, or severe); appearance of the mucosa (normal or rough); presence of mucopurulent exudate, fungal colonies (few or profuse), and foreign bodies; destruction of the nasal septum; and involvement of the frontal sinuses (involved or not involved) were assessed.

Data and statistical analyses—Radiographic, MRI, CT, and rhinoscopic findings were compared with respect to severity of lesions detected. All images were reviewed by a single investigator (JS), and rhinoscopy was performed by another investigator (CC). Assessment of the following features was compared among techniques: extent of lesions, degree of turbinate destruction, presence of abnormal soft tissue in the nasal cavity, lesions of bone surrounding the nasal cavities, and lesions of the frontal bone and sinuses. All variables were measured on an ordinal scale, and the Kruskal-Wallis test was used to compare techniques with respect to the degree of severity of lesions detected. Values of $P < 0.05$ were considered significant.

Unauthenticated | Downloaded 09/25/23 10:50 PM UTC

Results

Radiography—Radiographic lesions were detected in 14 of 15 dogs. The nasal cavities and frontal sinuses were involved in 9 dogs (unilaterally in 3 dogs and bilaterally in 6 dogs), and the nasal cavities alone were involved in 5 dogs (unilaterally in 4 dogs and bilaterally in 1 dog).

No turbinate destruction was detected in 1 dog, whereas the degree of turbinate destruction was minimal in 1 dog, moderate in 6 dogs, and severe in 7 dogs (**Figure 1**). No abnormal soft tissue was detected in the nasal cavities of 2 dogs, whereas the amount of abnormal soft tissue was minimal in 4 dogs, moderate in 5 dogs, and large in 4 dogs. A rim of soft tissue lining the nasal cavities (thickened mucosa) was detected in 10 dogs, and soft tissue at the nasofrontal ostium was detected in 10 dogs. A round soft tissue mass was detected in 3 dogs. The surrounding bone had a mixed pattern in 2 dogs; no lesions of the surrounding bone were detected in 13 dogs. Destruction of the bony portion of the nasal septum was evident in 7 dogs. Mineralization of contents of the nasal cavities, foreign bodies, and lysis of the cribriform plate were not detected.

The contents of the frontal sinuses were radiopaque in 9 dogs (**Figure 2**). Fluid could not be differentiated from soft tissue. The frontal bone had no lesions in 5 dogs, was hyperostotic in 6 dogs and lytic in 2 dogs, and had a mixed pattern in 2 dogs. Mineralization of contents of the frontal sinuses, round soft tissue masses, and extension of lesions to the periorbital region were not observed. The overall radiographic appearance was classified as cavitated in 13 dogs (Figure 1) and mass-like in 1 dog; 1 dog was considered normal.

MRI—Magnetic resonance imaging revealed lesions in all dogs. The nasal cavities and frontal sinuses were involved in 12 dogs, all parts of the nasal cavities were involved in 1 dog, and the rostral half of the nasal cavities was involved in 2 dogs. Involvement was unilateral in 6 dogs and bilateral in 9 dogs.

The degree of turbinate destruction was moderate in 8 dogs (**Figure 3**) and severe in 7 dogs. No abnormal soft tissue was detected in the nasal cavities of 1 dog, and the amount of soft tissue was minimal in 7 dogs, moderate in 6 dogs, and large in 1 dog. Thickened mucosa (a rim of soft tissue lining the nasal cavity) was detected in all dogs, and soft tissue at the nasofrontal ostium was detected in 12 dogs. A round soft tissue mass was revealed in 3 dogs. The surrounding bone had a mixed pattern in 1 dog, was hyperostotic in 1 dog, and had no lesions in 13 dogs. The nasal septum was destroyed in 8 dogs. Mineralization of contents of the nasal cavities, foreign bodies, and lysis of the cribriform plate were not observed.

The intensity of the nasal mucosa was enhanced in all dogs after contrast administration. Soft tissue intensities in the nasal cavities were enhanced in 14 dogs; this finding likely corresponded to inflamed mucosa on the remaining turbinates or the wall of the nasal cavity. In 2 dogs, a mass with heterogeneously enhanced intensity was detected. In another dog, a mass adjacent to the wall of the nasal cavity was hypointense (compared with normal nasal mucosa) on T1-weighted images, had no contrast enhancement of intensity, and was hypointense on T2-weighted images. These features were compatible with fungal colonies.

The frontal sinuses were involved in 12 dogs. A 2- to 3-mm-thick, hyperintense rim of soft tissue lining the frontal sinuses (thickened mucosa) was detected on

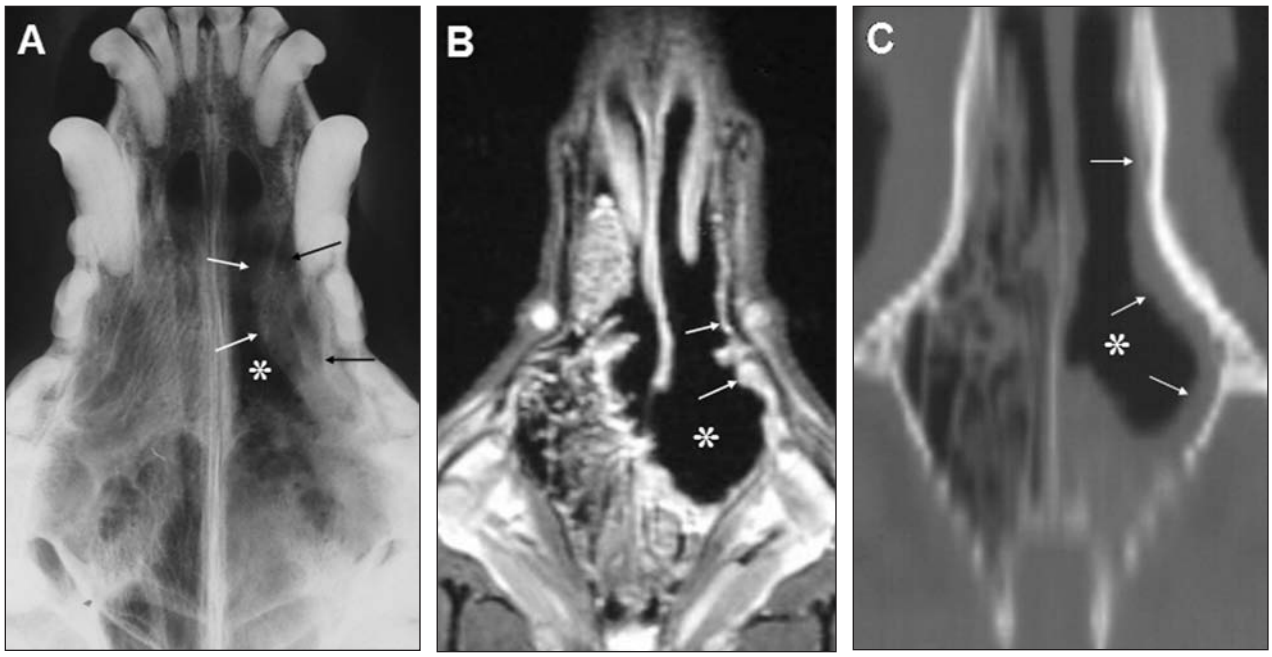

Figure 1—Images of the nasal cavities obtained via radiography, magnetic resonance imaging (MRI), and computed tomography (CT) in a dog with nasal aspergillosis. A—Dorsoventral (intraoral) radiographic view. B—Postcontrast T1-weighted dorsal plane magnetic resonance (MR) image. C—Computed tomographic dorsal reconstruction. Notice the cavitated appearance of the nasal cavity (asterisks) and the presence of a rim of soft tissue lining the nasal cavity (thickened mucosa; arrows).

Unauthenticated | Downloaded 09/25/23 10:50 PM UTC

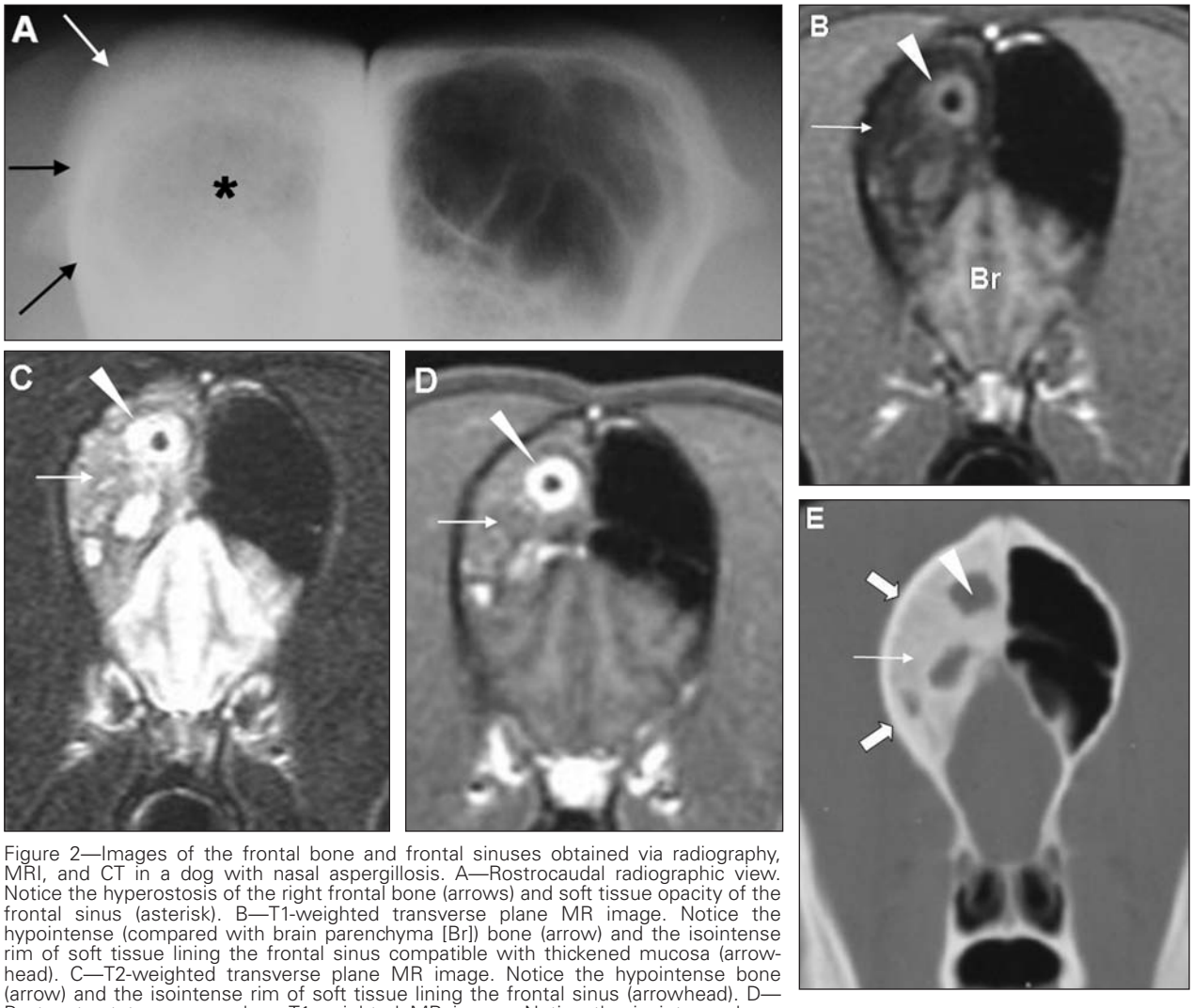

Figure 2—Images of the frontal bone and frontal sinuses obtained via radiography, MRI, and CT in a dog with nasal aspergillosis. A—Rostrocaudal radiographic view. Notice the hyperostosis of the right frontal bone (arrows) and soft tissue opacity of the frontal sinus (asterisk). B—T1-weighted transverse plane MR image. Notice the hypointense (compared with brain parenchyma [Br]) bone (arrow) and the isointense rim of soft tissue lining the frontal sinus compatible with thickened mucosa (arrowhead). C—T2-weighted transverse plane MR image. Notice the hypointense bone (arrow) and the isointense rim of soft tissue lining the frontal sinus (arrowhead). D—Postcontrast transverse plane T1-weighted MR image. Notice the isointense bone (arrow) and hyperintense rim of soft tissue lining the frontal sinus (arrowhead). E—Transverse plane CT image obtained with a bone window (window width = 3,500; window level = 500). Notice the severe hyperostosis of the frontal bone (small arrow). Cortical (large arrows) bone can be identified. A small amount of abnormal soft tissue is visible in the right frontal sinus (arrowhead).

T2-weighted images and postcontrast T1-weighted images in all of these dogs (**Figures 4 and 5**). Abnormal contents of the frontal sinuses were detected in 10 dogs (soft tissue and fluid in 9 dogs and a small amount of fluid in 1 dog). Variable soft tissue signal intensities were detected in the frontal sinuses; these were compared with the intensity of adjacent brain parenchyma. In 6 dogs, soft tissues were hypo- to isointense on T1-weighted images, had no contrast enhancement of intensity, and were hypointense on T2-weighted images. These features were consistent with chronically retained secretions or exudates, fungal colonies, or blood (acute hemorrhage). In 1 dog, the T1-weighted image features were similar; however, the pattern was hyperintense on T2-weighted images. All features for this dog were consistent with secretions with a high water or protein content, fungal colonies, a retention cyst, or polyposis. One dog had a heterogeneously intense soft tissue mass on all 3 (T1- and T2-weighted and postcontrast) images. Another dog had 2 round soft tissue masses in the frontal sinuses; 1 mass was isointense on T1-weighted images, had no contrast enhancement of intensity, and was hypointense on T2-weighted images. The other mass was isointense on T1-weighted images, had marked contrast enhancement of intensity, and was hyperintense on T2-weighted images.

No lesions of the frontal bone were found in 7 dogs; the frontal bone was hyperostotic in 5 dogs, was lytic in 1 dog, and had a mixed pattern in 2 dogs. The hyperostotic frontal bone was hypointense on T1-weighted images, was hypointense on T2-weighted images, and had moderate uptake of contrast medium (Figure 2). These features were consistent with chronic active osteomyelitis. The demarcation of osteomyelitic bone from cortical bone could still be made in most dogs. Extension of lesions to the periorbital region was detected in 1 dog, and a round soft tissue mass was detected in 2 dogs. A retention cyst in the unaffected contralateral frontal sinus was detected in 1 dog and was considered to be an incidental finding. The overall MRI appearance was classified as cavitated in all dogs (Figure 1).

Unauthenticated | Downloaded 09/25/23 10:50 PM UTC

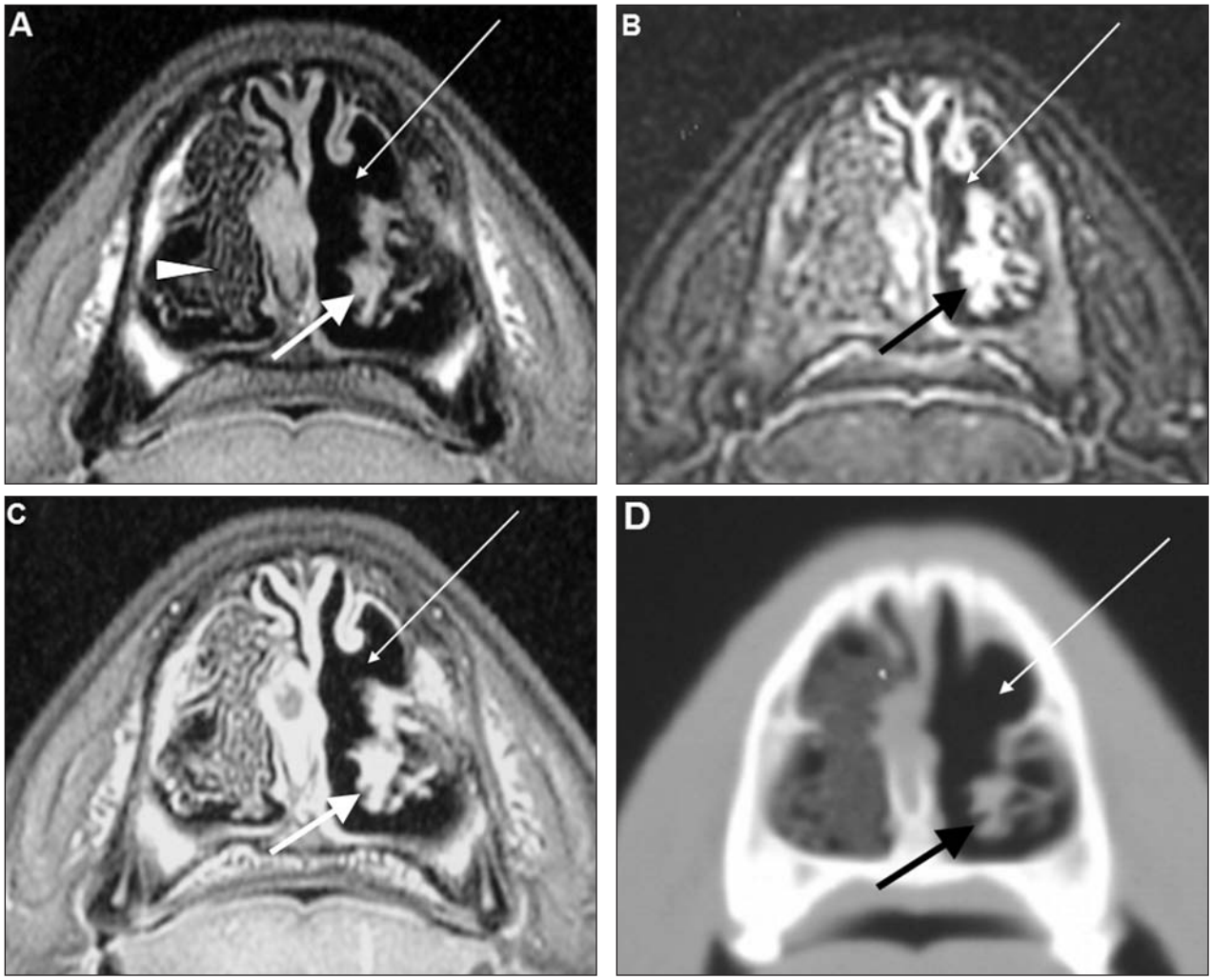

Figure 3—Images of the nasal cavities obtained via MRI and CT in a dog with nasal aspergillosis. Moderate destruction of the nasal turbinates in the left nasal cavity is evident (long arrow). A—T1-weighted transverse plane MR image. Notice the isointense (compared with normal nasal mucosa [arrowhead]) signal from the remaining turbinates (short arrow). B—T2-weighted transverse plane MR image. Notice the hyperintense signal from the remaining turbinates compatible with inflamed mucosa (short arrow). C—Postcontrast T1-weighted transverse plane MR image. Notice the moderate contrast enhancement of the remaining turbinates compatible with inflamed mucosa (short arrow). D—Computed tomography image in the transverse plane obtained with a bone window (window width = 3,500; window level = 500). Notice the abnormal soft tissue on the remaining turbinates (short arrow).

CT—Computed tomography revealed lesions in all dogs. The nasal cavities and frontal sinuses were involved in 12 dogs, all parts of the nasal cavities were involved in 1 dog, and the rostral half of the nasal cavities was involved in 2 dogs. Lesions were unilateral in 6 dogs and bilateral in 9 dogs.

Turbinate destruction was detected in all dogs (moderate destruction in 8 dogs and severe destruction in 7 dogs; Figures 1 and 3). Abnormal soft tissue was detected in the nasal cavities of 14 dogs (minimal amounts in 7 dogs, moderate amounts in 6 dogs, and large amounts in 1 dog), and a rim of soft tissue lining the nasal cavity (thickened mucosa) was detected in 14 dogs. It was not possible to differentiate between exudates and fungal colonies. Soft tissue at the nasofrontal ostium was detected in 12 dogs, and round soft tissue masses were detected in 3 dogs. Destruction of the nasal septum was evident in 8 dogs. No lesions of surrounding bone were detected in 6 dogs; bone was hyperostotic in 2 dogs and lytic in 3 dogs and had a mixed pattern in 4 dogs. Mineralization of contents of the nasal cavities, foreign bodies, and lysis of the cribriform plate were not observed. The intensity of soft tissue in the nasal cavities was enhanced in 14 dogs, most likely as a result of inflamed mucosa on the remaining turbinates or along the wall of the nasal cavity. In 2 dogs, the use of attenuation values allowed differentiation between nonvascularized and vascularized soft tissue; in 1 dog, a mass with heterogeneously enhanced intensity was detected, and in 1 dog, a mass adjacent to the nasal cavity wall had no contrast enhancement of intensity.

Lesions of the frontal sinuses were detected in 12 dogs (Figures 2, 4, and 5). In 2 dogs, a rim of soft tissue lining the frontal sinuses (thickened mucosa) was detected, and in 10 dogs, the mucosa was thickened and soft tissue or fluid was detected. Mucosal enhancement was revealed in only 1 dog via CT. It was possible to differentiate between thickened mucosa and abnormal soft tissue in 5 dogs; this was not accom-

Unauthenticated | Downloaded 09/25/23 10:50 PM UTC

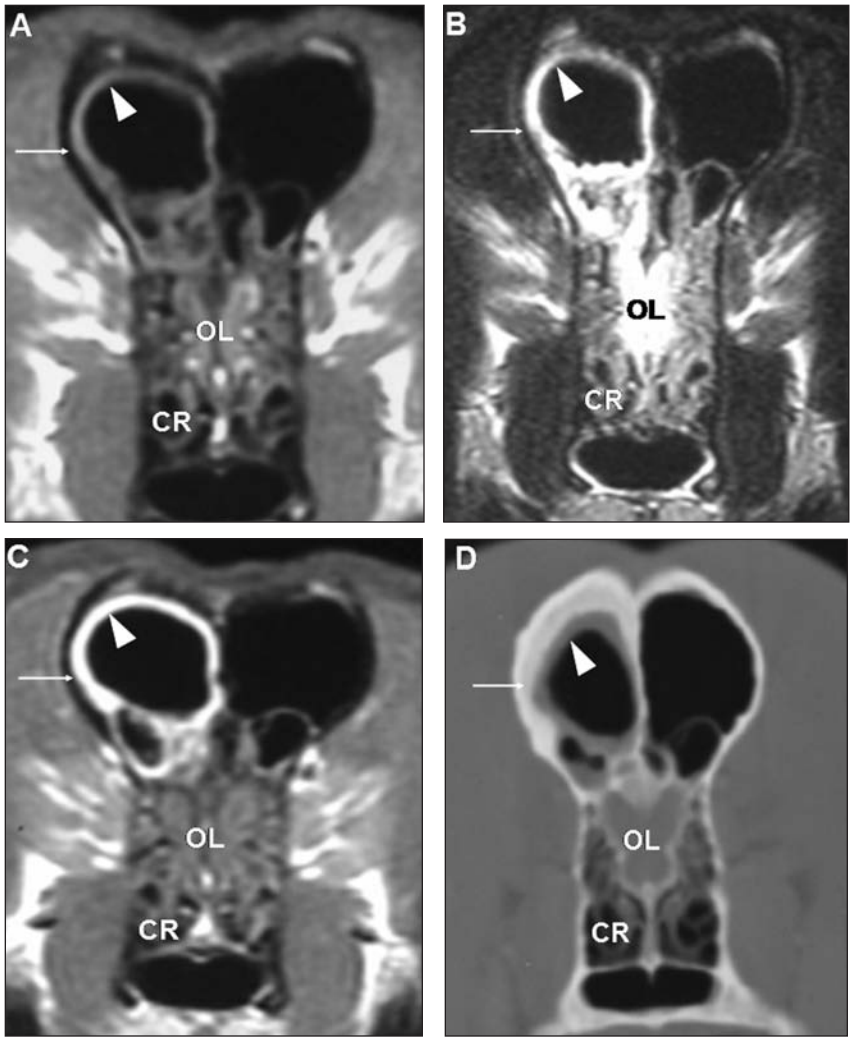

Figure 4—Images of the frontal sinuses and caudal nasal cavities obtained via MRI and CT in a dog with nasal aspergillosis. The olfactory lobe (OL), caudal recesses (CR = right caudal recess), and frontal bone (arrow) are evident on all images. A—T1-weighted transverse plane MR image. Notice the rim of soft tissue lining the frontal sinus (thickened mucosa) with an isointense (compared with the olfactory lobe) signal (arrowhead). The frontal bone has a signal void. B—T2-weighted transverse plane MR image. Notice that the rim of soft tissue lining the frontal sinus is isointense (arrowhead). C—Postcontrast T1-weighted transverse plane MR image. Notice the marked contrast enhancement (hyperintense signal) of the rim of soft tissue lining the frontal sinus (arrowhead). D—Computed tomography image in the transverse plane obtained with a bone window (window width = 3,500; window level = 500). Notice that the frontal bone is hyperostotic and consists of an outer layer of compact bone and an inner layer of cancellous bone. A rim of soft tissue lining the right frontal sinus is evident (arrowhead). Bone and soft tissue can easily be differentiated.

plished by use of attenuation values but by use of shape and location of the soft tissue. The nature of the soft tissue could not be determined even by use of attenuation values. No lesions of the frontal bone were detected in 4 dogs; the frontal bone was hyperostotic in 6 dogs and lytic in 1 dog and had a mixed pattern in 4 dogs. Extension of lesions to the periorbital region was detected in 1 dog, and a round soft tissue mass was detected in 3 dogs. Mineralization of contents of the frontal sinuses was not observed. The overall CT appearance was classified as cavitated in all dogs (Figure 1).

Rhinoscopy—Rhinoscopy revealed lesions in all dogs. The nasal cavities and frontal sinuses were involved in 11 dogs, all parts of the nasal cavities were involved in 2 dogs, and the rostral half of the nasal cavities was involved in 2 dogs. Abnormalities were unilateral in 9 dogs and bilateral in 6 dogs.

Fungal colonies were classified as profuse (**Figure 6**) in 12 dogs and few in 3 dogs. Turbinate destruction was detected in 15 dogs (minimal in 2 dogs and severe in 13 dogs). Mucopurulent exudate was detected in all dogs, and a rough mucosa was detected in 14 dogs. Destruction of the nasal septum was suspected in 6 dogs. Foreign bodies were not observed.

Comparison of techniques—Assessments of the extent of lesions detected with MRI and CT were similar. In 1 dog that had minimal destruction of the ventral nasal turbinates in 1 nasal cavity, no lesions were detected via radiography. Minimal lesions of the frontal sinuses (ie, small amount of fluid or focal lysis of the frontal crest) and destruction of the nasal septum were detected more frequently via MRI and CT than via radiography and rhinoscopy; however, significant differences in severity of lesions detected among techniques were found only for the lesions of bone surrounding the nasal cavities; the severity of these lesions assessed via CT was significantly ($P = 0.023$) higher than the severity assessed via radiography.

Agreement for the degree of turbinate destruction was 100% between MRI and CT and similar between MRI or CT and radiography. The amounts of abnormal soft tissue detected in the nasal cavities were assessed identically via MRI and CT. Seven dogs had a different classificaton of the amount of abnormal soft tissue assessed via radiography, compared with MRI and CT, but these differed by only a mild degree in 6 of 7 dogs. Thickened mucosa in the nasal cavities was detected in all dogs via MRI and 14 dogs via CT; however, mucosal thickening was suspected in only 10 dogs via radiography. Rhinoscopy was the only technique that allowed direct visualization and identification of abnormal soft tissue. A rough mucosa was observed in 14 dogs, and mucopurulent exudate and fungal colonies were observed in all dogs. Lesions in bone surrounding the nasal cavities were detected more frequently and with a higher level of confidence via CT than via radiography or MRI; via CT, bone lesions were detected in 9 dogs, whereas lesions were detected via MRI and radiography in only 2 severely affected dogs.

Unauthenticated | Downloaded 09/25/23 10:50 PM UTC

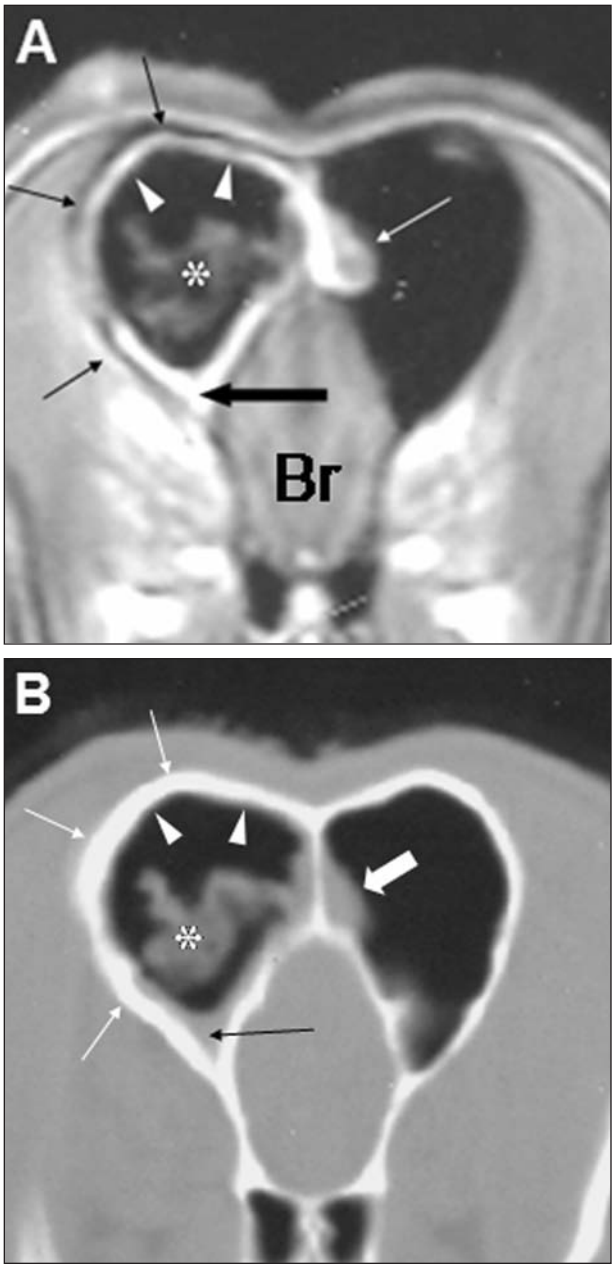

Figure 5—Images obtained at the level of the frontal sinuses via MRI and CT in a dog with nasal aspergillosis. A—Postcontrast T1-weighted transverse plane MR image. A hyperintense (strong contrast uptake) rim of soft tissue lining the right frontal sinus (thickened mucosa; arrowheads) is evident. Notice the hypointense (no contrast uptake) soft tissue mass in the right frontal sinus (asterisk). A small amount of fluid is evident in the ventral portion of the right frontal sinus (large black arrow) and an isointense (moderate contrast uptake) soft tissue mass in the medial compartment of the left frontal sinus (small white arrow) is present. The right frontal bone is slightly hypointense (small black arrows); an evaluation of the thickness of the bone is difficult because it cannot be compared with the left frontal bone that is normally a signal void. The intensities of the structures were compared with brain parenchyma (Br). B—Computed tomography image in the transverse plane obtained with a bone window (window width = 3,500; window level = 500). Notice the irregular soft tissue mass in the right frontal sinus (asterisk). A faint rim of soft tissue lining the right frontal sinus (arrowheads) is evident. The right frontal bone is moderately hyperostotic (small white arrows). A small amount of fluid in the ventral portion of the frontal sinus (small black arrow) and an oval soft tissue mass in the medial compartment of the left frontal sinus (large white arrow) are visible.

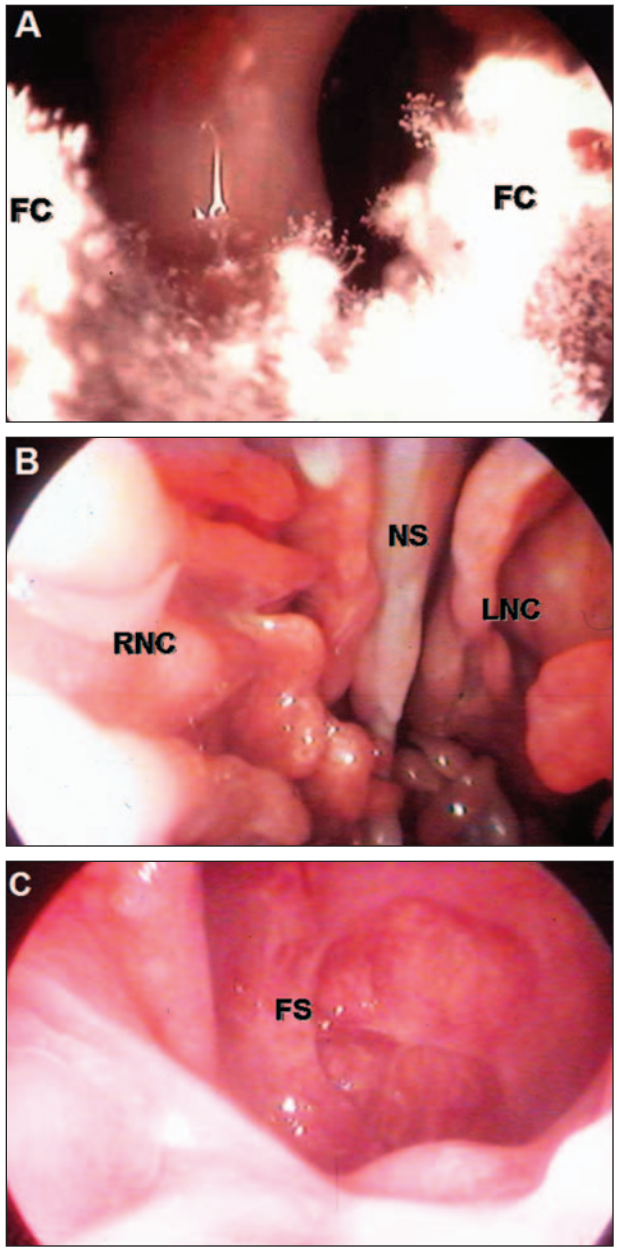

Figure 6—Rhinoscopic images in dogs with nasal aspergillosis. A—Rhinoscopic view of profuse intranasal fungal colonies (FC). B—Rhinoscopic view of the nasal cavities. Notice the severe destruction of the nasal septum (NS) allowing communication between the right (RNC) and left (LNC) nasal cavities. C—Rhinoscopic view of the frontal sinus (FS) in a dog after resolution of nasal aspergillosis. This view was possible as a result of extensive turbinate destruction that permitted access to the sinonasal ostium.

Minimal lytic and hyperostotic lesions were not detected via MRI. Compared with MRI and CT, rhinoscopy did not detect destruction of the nasal septum in 2 dogs and erroneously detected destruction in 1 dog.

On the basis of the CT findings for frontal sinuses, an incorrect diagnosis of presence of fluid or abnormal soft tissue was made in 5 dogs (1 false positive and 4 false negative) via radiography and in 3 dogs (1 false positive and 2 false negative) via rhinoscopy. Magnetic resonance imaging allowed differentiation between

Unauthenticated | Downloaded 09/25/23 10:50 PM UTC

mucosa and abnormal soft tissue in frontal sinuses of 10 dogs on the basis of signal intensity. Mucosal enhancement was revealed in only 1 dog via CT, and abnormal soft tissue was differentiated from mucosa on the basis of the shape and location of the soft tissue in 5 dogs; however, it was not possible to identify the nature of soft tissue either via MRI or CT. Lesions of the frontal bone were best detected via CT; however, the same diagnosis (normal and abnormal bone) was made in 12 and 13 dogs via MRI and radiography, respectively. Extension of lesions to the periorbital region detected in 1 dog via MRI and CT was not detected via radiography.

Discussion

Imaging studies should be performed prior to rhinoscopy and biopsy procedures because the resultant hemorrhage may obscure subtle lesions and induce imaging abnormalities. Because we wished to confirm a diagnosis of nasal aspergillosis prior to imaging studies, rhinoscopy was performed initially. During rhinoscopic examination, gentle manipulation of the endoscope was used to minimize iatrogenic damage and hemorrhage.

Magnetic resonance imaging and CT were the most useful techniques for evaluation of the extent of lesions (including unilateral and bilateral involvement and destruction of the nasal septum). The MRI and CT techniques avoid superimposition of anatomic structures; therefore, the image is less complex than a radiograph and gives a simpler view of lesions.[16] Radiographic evaluation of a diseased nasal cavity is difficult because of the superimposition of bony structures and the complexity of the nasal turbinates.[19,20] Some nasal structures are never (nasal septum and caudal recesses) or not always (orbital lamina of the maxillary recesses) visible via radiography, whereas others are detected only when they are destroyed (cribriform plate, naso-orbital wall, and vomer bone).[21-23] When an appropriate technique is used, radiography is a good imaging method for detection of opacification of nasal cavities and frontal sinuses, except when lesions are bilateral and subtle.[19,20,24-26] In our study, radiography did not detect frontal sinus involvement in 2 dogs that had mucosal thickening and a small amount of fluid in the lateral compartment of the frontal sinuses via MRI. Minimal destruction of the turbinates in the ventrorostral third of 1 nasal cavity in 1 dog was detected via MRI and CT but not via radiography. Removal of the turbinates and replacement with gelatin results in detectable radiographic changes when radiographs are of good quality.[21] To the authors' knowledge, the minimal amount of destruction of the rostral turbinates that is necessary for detection via radiography is not known; however, detection is dependent on the quality of the radiograph.[26] Rhinoscopy does not allow evaluation of bony structures, and extensive turbinate destruction must be present before the frontal sinuses and cribriform plate can be seen.[7,27] In our study, radiography and rhinoscopy did not reveal nasal septum destruction and extension of lesions to the contralateral medial frontal sinus in 1 dog, suggesting that in dogs in which MRI or CT is not performed, both nasal cavities and frontal sinuses should be treated.

Radiography was a valuable technique for evaluation of the amount of soft tissue in the nasal cavities; however, with the exception of detection of a rim of soft tissue lining the nasal cavities, suggesting a thickened mucosa, radiography did not allow identification of the nature of soft tissue opacities. Via CT, the intranasal and intrasinusal tissue could be differentiated from bone; however, the nature of the abnormal soft tissue could not be identified with a high level of confidence even when soft tissue window settings were used. Theoretically, use of attenuation measurements may permit differentiation between mucosa and abnormal soft tissue or fluid or between necrotic and vascularized soft tissue; however, this differentiation could only be achieved in 2 dogs in our study. Attenuation measurements are susceptible to a variety of errors in diseased nasal cavities mainly because of the presence and occasional mixing of many complex structures of variable physical density; the equivalent range of enhanced values of normal, inflamed, and neoplastic tissue; and the presence of mucoid secretions and fungal colonies that have attenuation values that fall within the same range of Hounsfield units.[28,29]

With the use of different sequences, MRI has substantially improved relative contrast between normal and abnormal soft tissue and may therefore aid in the identification of diseases of the nasal cavities and frontal sinuses.[30] Normal sinonasal secretions comprise a complex solution in equilibrium with interstitial fluid. Initially aqueous (low T1-weighted signal and high T2-weighted signal), these secretions change to a thick mucus (low T1-weighted signal and low T2-weighted signal) or desiccated plugs (signal voids on T1- and T2-weighted images) if they cannot be removed.[31,32] This occurs in chronically obstructed frontal sinuses in dogs with nasal aspergillosis. Other factors that influence the signal intensity of secretions in obstructed frontal sinuses in a similar manner are the cross-linking and polymerization of macromolecular glycoproteins and an increase in viscosity.[32,33] Fungal colonies generate low T1- and T2-weighted signal intensities or even signal voids.[31,34,35] This is believed to be the result of the combined presence of metal ions (iron and manganese) that are essential elements in fungal amino acid metabolism and calcium salt deposits (endogenous fungal products) in necrotic areas of the mycelium.[30,34] Because of the possible signal overlap between secretions and fungal colonies and because there is no way to predict prior to cross-sectional imaging how desiccated secretions will be, differentiation between secretions and fungal colonies is not possible. Mineralized contents of nasal cavities and frontal sinuses were not observed in our dogs via CT, and signal void zones on T2-weighted MR images were also not observed.

Comparison with rhinoscopic images allowed identification of fungal colonies in the nasal cavity of 1 dog via MRI. The fungal colonies revealed a low intensity signal on T1- and T2-weighted images and no contrast uptake. These features were also observed in the frontal sinuses of 6 dogs via MRI. In these dogs, fungal colonies were detected in the frontal sinuses via rhinoscopy; however, exudates were also found. In

Unauthenticated | Downloaded 09/25/23 10:50 PM UTC

contrast to the 3 imaging techniques, rhinoscopy allows identification of soft tissue via direct visualization. Rhinoscopy allows evaluation of the mucosa, nature of the content of the nasal cavities and sinuses (mucoid secretions, purulent debris, blood, and foreign bodies), appearance of the turbinates (absence, swelling, change in color, and atrophy), and presence of etiologic agents (fungal colonies and parasites) or masses (polypoid masses, neoplasms, cysts, and granulomas).[7,27,36,37] The macroscopic appearance of fungal colonies via rhinoscopy varies with time; however, fungal colonies can only be confused with mucopurulent exudate at an early stage of the disease by inexperienced observers.[7]

In our study, CT and MRI allowed for more accurate and easier detection of a thickened mucosa and fluid or abnormal soft tissue in the frontal sinuses and frontal bone lesions, compared with rhinoscopy and radiography. A rim of soft tissue lining the frontal sinuses (thickened mucosa) and hyperostotic bone are CT and MRI features strongly suggestive of nasal aspergillosis.[9] The frontal sinuses are air-filled structures that provide a high natural contrast between air and soft tissue and between soft tissue and bone (amounts to at least 700 to 1,000 Hounsfield units). In a previous study[8] by the authors, it was suggested that the absence of enhancement of the mucosa in the frontal sinuses on postcontrast CT studies could have been caused by hypertrophic, hyperplastic, and fibrotic changes of the sinusal mucosa. This is in contrast to results of the present study in which sinusal mucosal enhancement was observed in all dogs with frontal sinus involvement via MRI. The absence of mucosal enhancement in the frontal sinuses via CT in the previous study could have been the result of the presence of a thin mucosa that prevented differentiation from bone on a soft tissue window, whereas the contrast uptake could not be visualized on a bone window.

Computed tomography was the best technique for evaluation of cortical bone lesions in the bone surrounding the nasal cavity. These lesions nearly always consisted of minimal bone hyperostosis, lysis, or both. Computed tomography was also the best technique for detection of lesions of the frontal bone. The lesions in the frontal bone (predominantly hyperostosis) were more severe than those in the bone surrounding the nasal cavities; therefore, MRI and radiography also allowed evaluation of frontal bone. Magnetic resonance imaging is insensitive for recognition of cortical bone in which hydrogen protons are immobile and produce a signal void that cannot be differentiated from that of air, desiccated secretions, mycetomas, acute hemorrhage, calcium, and enamel[38]; however, MRI provides high contrast among abnormal bone marrow, normal bone marrow, and cortical bone.[39] The signal intensities observed in hyperostotic frontal bone in our study (low signal intensity on T1-weighted images, low signal intensity on T2-weighted images, and moderate contrast enhancement) corresponded to those described in humans with osteomyelitis.[39,40]

Computed tomography and MRI are more useful than radiography for evaluation of the integrity of the cribriform plate, extension of lesions to the periorbital region, and presence of an associated intranasal (eg, neoplasia or foreign body) or extranasal (eg, tooth abscess or neoplasia) disease process.[41] We could not confirm these conclusions in our study because there were no dogs with lesions of the cribriform plate or with an associated disease process. Extension of lesions to the periorbital region detected in 1 dog via CT and MRI was not detected via radiography or rhinoscopy.

One limitation of our study was the lack of an independent gold standard (ie, surgical exploration) with which the results of radiography, CT, and MRI could be compared objectively. This would have been particularly useful in dogs in which lesions were detected via MRI and CT but were not detected via radiography; however, CT and MRI consistently revealed a greater number of lesions than radiography. The interpretation of MRI findings was difficult because of the lack of experience of the observers, absence of histologic examination of the intrasinusal soft tissue, and the complexity of intranasal and intrasinusal material. Another limitation of our study was the small number of dogs (3) with lesions restricted to the nasal cavities. The diagnosis of nasal aspergillosis is challenging in such dogs.[9]

Magnetic resonance imaging and CT revealed features strongly suggestive of nasal aspergillosis more frequently than did radiography. The higher sensitivity of CT versus radiography was observed in a previous study.[9] Once a diagnosis is made, however, the complementary findings via MRI or CT do not influence or modify the treatment protocol for nasal aspergillosis.[42] On the basis of the results of our study, the most appropriate protocol for diagnosis of nasal aspergillosis appears to be CT or MRI followed by rhinoscopy.

[a]Sharp NJH, Harvey CE, Sullivan M. Sequential serology in canine nasal aspergillosis (abstr), in *Proceedings*. 5th Annu Am Coll Vet Int Med Forum 1987;915.

[b]Sharp NJH, Harvey CE, Sullivan M. Treatment of canine nasal aspergillosis (abstr), in *Proceedings*. 5th Annu Am Coll Vet Int Med Forum 1987;916.

[c]Cystoscope K Storz SL 30° Ref BA 3059308, Karl-Storz-Endoscopy America Inc, Culver City, Calif.

[d]Fujinon EB-4105, Onys SA, Brussels, Belgium.

[e]Prestilix, GE Medical Systems, Milwaukee, Wis.

[f]Agfa-Gevaert NV, Ridgefield Park, NJ.

[g]MAGNETOM Symphony, Siemens, Malvern, Penn.

[h]Signa, GE Medical Systems, Milwaukee, Wis.

[i]Magnevist, Schering, Kenilworth, NJ.

[j]Picker 6000, Picker, Eastlake, Ohio.

[k]Omnipaque 300, Nycomed, Brussels, Belgium.

References

1. Sharp NJH, Harvey CE, Sullivan M. Canine nasal aspergillosis and penicilliosis. *Compend Contin Educ Pract Vet* 1991;13:41–49.

2. Gartrell CL, O'Handley PA, Perry RL. Canine nasal disease—part II. *Compend Contin Educ Pract Vet* 1995;17:539–547.

3. Sharp NJH. Aspergillosis and penicilliosis. In: Greene CE, ed. *Infectious diseases of the dog and cat*. 2nd ed. Philadelphia: WB Saunders Co, 1998;404–409.

4. Wolf AM. Fungal diseases of the nasal cavity of the dog and cat. *Vet Clin North Am Small Anim Pract* 1992;22:1119–1132.

5. Sharp NJH, Sullivan M, Harvey CE. Treatment of canine nasal aspergillosis. *In Pract* 1992;14:27–31.

6. Sullivan M, Lee R, Jakovljevic S, et al. The radiological features of aspergillosis of the nasal cavity and frontal sinuses in the dog. *J Small Anim Pract* 1986;27:167–180.

Unauthenticated | Downloaded 09/25/23 10:50 PM UTC

7. McCarthy TC, McDermaid SL. Rhinoscopy. *Vet Clin North Am Small Anim Pract* 1990;20:1265–1290.

8. Saunders JH, Zonderland JL, Clercx C, et al. Computed tomography of 35 dogs with nasal aspergillosis. *Vet Radiol Ultrasound* 2002;43:5–9.

9. Saunders JH, van Bree H. Comparison of radiography and computed tomography for diagnosis of canine nasal aspergillosis. *Vet Radiol Ultrasound* 2003;44:414–419.

10. Lloyd GAS, Lund VJ, Phelps PD, et al. Magnetic resonance imaging in the evaluation of nose and paranasal sinus disease. *Br J Radiol* 1987;60:957–968.

11. Som PM, Dillon WP, Curtin HD, et al. Hypointense paranasal sinus foci: differential diagnosis with MR imaging and relation to CT findings. *Radiology* 1990;176:777–781.

12. Chong VFH, Fan YF. Comparison of CT and MRI features in sinusitis. *Eur J Radiol* 1998;29:47–54.

13. Hudson LC, Cauzinille L, Kornegay JN, et al. Magnetic resonance imaging of the normal feline brain. *Vet Radiol Ultrasound* 1995;36:267–275.

14. Vernau KM, Kortz GD, Koblik PD, et al. Magnetic resonance imaging and computed tomography characteristics of intracranial intra-arachnoid cysts in 6 dogs. *Vet Radiol Ultrasound* 1997;38:171–176.

15. Dennis R. Magnetic resonance imaging and its application in small animals. *In Pract* 1998;20:117–124.

16. Forrest LJ. The head: excluding the brain and orbit. *Clin Tech Small Anim Pract* 1999;14:170–176.

17. Moore MP, Gavin PR, Kraft SL, et al. MR, CT and clinical features from four dogs with nasal tumors involving the rostral cerebrum. *Vet Radiol Ultrasound* 1991;32:19–25.

18. Voges AK, Ackerman N. MR evaluation of intra- and extracranial extension of nasal adenocarcinoma in a dog and cat. *Vet Radiol Ultrasound* 1995;36:196–200.

19. Thrall DE, Robertson ID, McLeod DA, et al. A comparison of radiographic and computed tomographic findings in 31 dogs with malignant nasal cavity tumors. *Vet Radiol Ultrasound* 1989;30:59–66.

20. Park RD, Beck ER, LeCouteur RA. Comparison of computed tomography and radiography for detecting changes induced by malignant neoplasia in dogs. *J Am Vet Med Assoc* 1992;201:1720–1724.

21. Schmidt M, Voorhout G. Radiography of the canine nasal cavity: significance of the presence or absence of the trabecular pattern. *Vet Radiol Ultrasound* 1992;33:83–86.

22. Schwarz T, Sullivan M, Hartung K. Radiographic anatomy of the cribriform plate (lamina cribrosa). *Vet Radiol Ultrasound* 2000; 41:220–225.

23. Schwarz T, Sullivan M, Hartung K. Radiographic detection of defects of the nasal boundaries. *Vet Radiol Ultrasound* 2000; 41:226–230.

24. Gibbs C, Lane JG, Denny HR. Radiological features of intranasal lesions in the dog: a review of 100 cases. *J Small Anim Pract* 1979;20:515–535.

25. Sullivan M, Lee R, Skae CA. The radiological features of sixty cases of intra-nasal neoplasia in the dog. *J Small Anim Pract* 1987;28:575–586.

26. Miyabayashi T, Biller DS, Haider PR, et al. Radiographic appearances of the nasal conchae in dogs using different screen-film systems: a postmortem study. *J Am Anim Hosp Assoc* 1994;30:382–388.

27. Noone KE. Rhinoscopy, pharyngoscopy, and laryngoscopy. *Vet Clin North Am Small Anim Pract* 2001;31:671–689.

28. Williams G, Bydder GM, Kreel L. The validity and use of computed tomography attenuation values. *Br Med Bull* 1980;36:279–287.

29. Mathews KG, Koblik PD, Richardson EF, et al. Computed tomographic assessment of noninvasive intranasal infusions in dogs with fungal rhinitis. *Vet Surg* 1996;25:309–319.

30. Fellows DW, King VD, Conturo T, et al. In vitro evaluation of MR hypointensity in *Aspergillus* colonies. *AJNR Am J Neuroradiol* 1994;15:1139–1144.

31. Som PM, Dillon WP, Fullerton GD, et al. Chronically obstructed sinonasal secretions: observations on T1 and T2 shortening. *Radiology* 1989;172:515–520.

32. Som PM, Curtin HD. Chronic inflammatory sinonasal diseases including fungal infections. The role of imaging. *Radiol Clin North Am* 1993;31:33–44.

33. Dillon WP, Som PM, Fullerton GD. Hypointense MR signal in chronically inspissated sinonasal secretions. *Radiology* 1990;174:73–78.

34. Zinreich SJ, Kennedy DW, Rosenbaum AE, et al. Paranasal sinuses: CT imaging requirements for endoscopic surgery. *Radiology* 1987;163:769–775.

35. Zinreich SJ, Kennedy DW, Malat J, et al. Fungal sinusitis: diagnosis with CT and MR imaging. *Radiology* 1988;169:439–444.

36. Venker-Van Haagen AJ, Van Oosterhout ICAM, Meij BP, et al. L'examen rhinoscopique en clinique des petits animaux: analyse des résultats de 233 rhinoscopies. *Prat Med Chir Anim Comp* 1990;25:79–87.

37. Lent SE, Hawkins EC. Evaluation of rhinoscopy and rhinoscopy-assisted mucosal biopsy in diagnosis of nasal disease in dogs: 119 cases (1985–1989). *J Am Vet Med Assoc* 1992;201:1425–1429.

38. Zimmerman RA, Bilaniuk LT, Hackney DB, et al. Paranasal sinus hemorrhage: evaluation with MR imaging. *Radiology* 1987;162: 499–503.

39. Tehranzadeh J, Wong E, Wang F, et al. Imaging of osteomyelitis in the mature skeleton. *Radiol Clin North Am* 2001;39:223–250.

40. Hopkins KL, Li KC, Bergman G. Gadolinium-DTPA-enhanced magnetic resonance imaging of musculoskeletal infectious processes. *Skeletal Radiol* 1995;24:325–330.

41. Koblik PD, Berry CR. Dorsal plane computed tomographic imaging of the ethmoid region to evaluate chronic nasal disease in the dog. *Vet Radiol Ultrasound* 1990;31:92–97.

42. Davidson AP, Mathews KG, Koblik PD, et al. Diseases of the nose and nasal sinuses. In: Ettinger SJ, ed. *Textbook of veterinary internal medicine*. 5th ed. Philadelphia: WB Saunders Co, 2000;1003–1025.

Unauthenticated | Downloaded 09/25/23 10:50 PM UTC